Gaussian distribution of inhomogeneous Barrier Height in Au/n-GaP (100) Schottky Barrier diodes

M. ÖZER[a], T. GÜZEL[a], A. ASIMOV[b], M. AHMETOGLU (AFRAİLOV)[b,*]
[a]*Physics Department, Faculty of Arts and Sciences, Gazi University,Teknikokullar, 06500 Ankara, Turkey*
[b]*Department of Physics, Faculty of Sciences and Arts, Uludag University, 16059Gorukle, Bursa, Turkey*

The current–voltage (I–V) measurements of Au/n-GaP Schottky barrier diodes (SBD) were carried out in the temperature range of 80–375 K. The values of zero-bias barrier height (ϕ_{B0}) and ideality factor (n) ranged from 0.29 eV and 3.85 (80K) to 0.82 eV and 1.16 (375K), respectively. Such behavior of ϕ_{B0} and n is attributed to Schottky barrier inhomogeneities by assuming a Gaussian Distribution (GD) of barrier hights (BHs) at Au/n-GaP interface. The ϕ_{B0} vs $q/(2kT)$ plot has been drawn to obtain evidence of a Gaussian distribution of the barrier heights,and values of ϕ_{B0}= 0,97 eV and σ_0 = 0.10 V for the mean barrier height and zero-bias standard deviation have been obtained from this plot, respectively. Thus a modified ln (I_0/T^2) - $q^2\sigma_o^2/2k^2T^2$vs 1000/T plot has given mean barrier height ϕ_{B0} and Richardson constant (A^*) as 1.95 eV and 0.054 A cm^{-2} K^{-2}, respectively. The temperature dependence of the *I–V* characteristics of the Au/n-GaP Schottky diode have been successfully explained on the basis of thermionic emission (TE) mechanism with GD of the Schottky barrier heights (SBHs).

(Received August 26, 2013; accepted May 15, 2014)

Keywords: Schottky contacts, Schottky Barrier Height, Gaussian Distribution Inhomogeneities

1. Introduction

Schottky barriers formed by metal–semiconductor contact have been widely studied. They are important research tools in the characterization of new semiconductor materials and at the same time the fabrication of these structures play acrucial role in constructing some useful devices in technology. The performance and reliability of a Schottky diode is drastically influenced by the interface quality between the deposited material and the semiconductor surface. Due to the technological importance of SBDs, a full understanding of the nature of their current–voltage(I-V) and capacitance–voltage (C–V) characteristics is of greater interest[1-6]. The most important feature characterizing a Schottky barrier is its barrier height. Several theories exist, which however can explain only some of the experimental facts. Therefore, there is a need fornew experiments, which may yield more insight into the mechanisms determining ϕ_{B0}. The spatial variation of barrier heights in inhomogeneous Schottky diodesis described mainly by the GD function. In the past, the GD of barrier heights has been widely accepted to correlate experimental data [1-18]. Generally, the TE theory uses the SBD parameters and the ideality factor that is expected to be close to unity [19-20]. However, analysis of the forward bias I–V characteristics of SBDs based on TE theory usually reveals an abnormal decrease in the SBH and an increase in the ideality factor n with a decrease in temperature [3-6,21-25]. The decrease in the barrier height at low temperatures leads to non-linearity in the activation energy $\ln(I_0/T^2)$ versus $1/T$ plot. Nowadays, the nature and origin of the decrease in the BH and increase in ideality factor with a decrease in temperature in some studies [1-18] have been successfully explained on the basis of a TE mechanism with GD of the BHs. In this report, we present I–V–T measurements inthe temperature range 80–375K on inhomogeneous Au/n-GaPSBDs. The temperature dependence of the BH and the ideality factoris discussed using TE theory with GDof the BHs around a mean value due to barrier height inhomogeneities prevailing at the metal–semiconductor interface.

2. Experimental

Au/n-GaP SBDs were fabricated on 2 inch diameter float zone (100) n-type (S doped) single crystal GaP wafer having thickness of 300 μm. Before making contacts, the GaP wafer was degreased for 5 min in boiling trichloroethylene, acetone and methanol, consecutively. After chemically etched using the RC cleaning procedure with (DIH_2O:H_2O_2:NH_4OH:5:1:1) solution for 5 min, the native oxide layer on the front surface ofthe substrate was removed in DIH_2O:HF (100:1) solution and finallythe wafer was rinsed in (DIH_2O:H_2O_2:HCl:6:1:1) for 30 s, and then rinsed in deionized water of resistivity of 18 MΩ cm with ultrasonic vibration and dried by high purity nitrogen. Immediately after surface cleaning, the high purity gold (Au) and germanium (Ge) metal (99.999%), respectively, with a thickness of 2000 A^0 were thermally evaporated from tungsten filament onto the whole back surface of the

GaP wafers at apressure of ≈10^{-6}in liquid nitrogen trapped oil-free ultra high vacuum pump system. To obtain a low-resistivitiy ohmic back contact, both evaporated Au and Ge back contact GaP wafers were sintered in vacuum at about 400 ^{o}C and 3 min in N_2 atmosphere. Immediately after ohmic contact, circular dots shaped Au Schottky (rectifier) contacts with diameter of about 1.5 mm and 2500A^0 thickness were formed by evaporating Au in the pressure of ≈10^{-6} Torr. The temperature dependence of I–V measurements were performed by the use of a Keithley 6517A electrometer in the temperature range of 80–375 K using a temperature-controlled Janes vpf-475 cryostat. The sample temperature was always monitored by using a copper-constant thermocouple close to the sample, and measured with admm/scanner Keithley model 19 and a Lake Shore model 321 auto-tuning temperature controllers with sensitivity better than ±0,1K. All measurements were carried out with the help of a micro computer through an IEEE-488 ac/dc converter card.

3. Results and discussion

3.1. The current–voltage characteristics as a function of temperature

The I–V relation for a metal-semiconductor (MS) diode,based on the TE theory can be expressed as [13,19].

$$I = I_0 \exp\left(\frac{qV}{nkT}\right)\left[1-\exp\left(\frac{-qV}{kT}\right)\right] \quad (1)$$

where I is the measured current, V is the applied voltage, q is the electronic charge, n is the ideality factor that describes the deviation from the ideal diode equation for reverse bias as well as forward bias, k is theBoltzmann's constant, T is the absolute temperature in Kelvin, I_0 is the saturation current derived from the straight line intercept of $ln\ I$ at zero-bias and is given by

$$I_0 = AA^*T^2 \exp\left(-\frac{q\phi_{B0}}{kT}\right) \quad (2)$$

where A,A^*,T, q,k and $\phi_{B0}$are the diode area, the effective Richardson constant of 50 A $K^{-2}cm^{-2}$ for n-type GaP [26], temperature in K, the electronic charge, Boltzmann's constant and the zero-biasbarrier height, respectively. The ϕ_{B0}can be obtained from Eq. (2)

$$\phi_{B0} = \frac{kT}{q}\ln\left(\frac{AA^*T^2}{I_0}\right) \quad (3)$$

Table 1. Temperature dependent values of various diode parameters determined from I–V characteristics of Au/n-GaP Schottky barrier diodes in the temperature range of 80–375 K.

T(K)	n	Io(A)	Φ_B(I-V)(eV)
80	3.85	8.08E-19	0.29
100	3.01	3.38E-19	0.37
125	2.38	5.10E-19	0.47
150	2.02	2.13E-18	0.54
175	1.82	2.60E-17	0.6
200	1.62	1.34E-16	0.66
225	1.47	1.03E-15	0.71
250	1.39	1.03E-14	0.75
275	1.33	1.10E-13	0.77
300	1.23	1.16E-12	0.78
325	1.17	4.72E-12	0.79
350	1.20	7.02E-11	0.80
375	1.16	2.31E-10	0.82

The ideality factor is determined from the slope of the linear region of the plot of natural log of forward current vs. forward bias voltage and is given by

$$n = \frac{q}{kT}\left(\frac{dV}{d(\ln I)}\right) \quad (4)$$

Fig. 1 shows the semilog I–V characteristics of the Au/n-GaP Schottky diodes at different temperatures. We have performed least square fits of Eq. (1) to the linear part of the measured I–V plots (Fig. 1). From these fits, theexperimental values of n andϕ_{B0}were determined from intercepts and slopes of the forward bias $ln\ I$ versus V plot at each temperature, respectively. Once I_0 is known, the zero bias barrier height can be computed with the help of Eq. (2). The $\phi_{B0}$and determined from semilog-forward I–V plots were found to be a strong function of temperature.

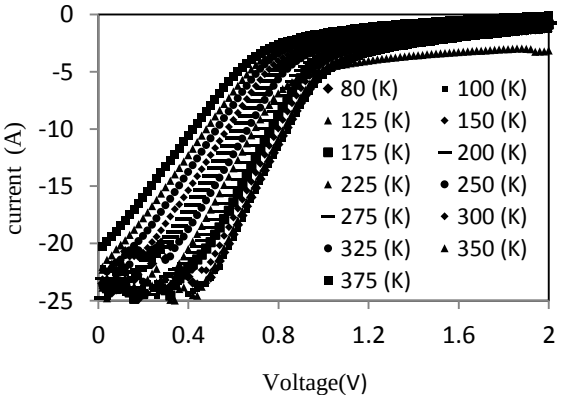

Fig. 1. Experimental forward-bias current–voltage characteristics of Au/n-GaP Schottky diode at different temperatures.

The zero-bias barrier height ϕ_{B0} values which were calculated at each temperature from Eq. (3) based on pure

TE are shown in Table 1 and Fig. 2 at various temperatures. The experimental values of ϕ_{B0} and n were changed from 0.29 eV and 3.85 (at 80 K) to 0.82 eV and 1.16 (at 375 K). As seen in Table 1, while the ideality factor decreases with increasing temperature the zero-bias barrier height increases with increasing temperature. The temperature coefficient β of barrier height is calculated 1.7 meV (Fig. 2). This temperature dependence is an obvious disagreement with the reported negative temperature coefficient of ϕ_{B0}. Moreover the value of ϕ_{B0} at 0 K is found to be 0.24 eV (Fig. 2).

The ideality factor of an inhomogeneous SBD with a distribution of low BHs may increase with a decrease in temperature. It has been report that there is a linear correlation between the experimental zero-bias barrier heights ϕ_{B0} and the ideality factors n [15,25]. Fig. 2 shows the plot of the experimental BH versus the ideality factor for various temperatures. As can be seen in this figure the BHs become smaller as the ideality factors increase.

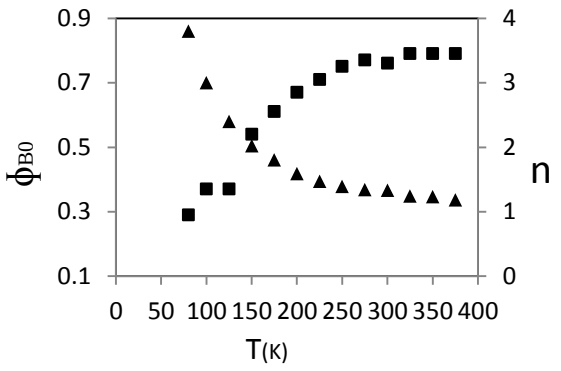

Fig. 2. The variation in the ideality factor and zero-bias barrier height with temperature for Au/n-GaP (SBD).

The straight line in Fig. 3 is the least squares fit to the experimental data. That is, there is a linear relationship between experimental effective BHs and ideality factors of Schottky contacts. The extrapolation of the experimental BHs versus ideality factor plot to n=1 has given a homogeneous BH of approximately 0.85 eV. Thus, it can be said that the significant decrease of the zero-bias BH and increase of the ideality factor especially at low temperature are possibly caused by the BH inhomogeneities [28-31].

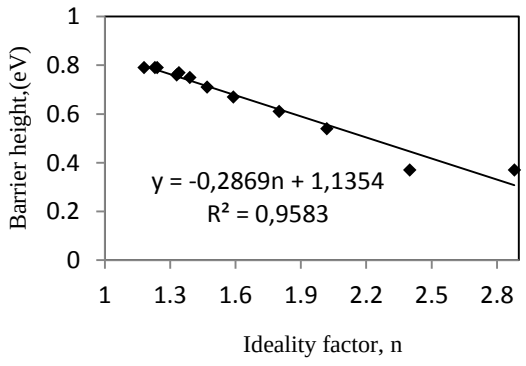

Fig. 3. Zero-bias barrier height vs. ideality factor of a typical Au/n-GaP Schottky diode at different temperatures.

The barrier height, which decreases with decreasing temperature, obtained from Eq. (2) is called apparent or zero-bias barrier height. The barrier height obtained under flat-band condition is called flat-band barrier height and is considered to be real fundamental quantity. Unlike the case of the zero-bias barrier height, the electrical field in the semiconductor is zero under the flat-band condition. This eliminates the effect of the image force lowering that would affect the I–V characteristics and removes the influence of lateral inhomogeneity [10]. The flat-band barrier height is given by [8]

$$\Phi_{bf} = n\Phi_{bo} - (n-1)\left(\frac{kT}{q}\right)\ln\left(\frac{Nc}{Nd}\right) \tag{5}$$

where N_c is the effective density of states at the conduction band and N_d is the donor concentration. The C–V measurements have been performed at 1 MHz in the temperature range of 80–375K. The experimental N_c and N_d depending on the temperature were calculated from the reverse bias C^{-2}–V characteristics. The values of N_c and N_d are $2.70\text{x}10^{18}\text{cm}^{-3}$ at 80 K and $2.96\text{x}10^{18}\text{cm}^{-3}$ at 300 K,and $1.96\text{x}10^{19}\text{cm}^{-3}$ at 80 K and $2.98\text{x}10^{18}\text{cm}^{-3}$ at 300 K, respectively. The N_c and N_d of the n-GaP decreased slightly with a decrease in temperature inthe temperature range of 80–375 K. Fig. 4 shows the variation of Φ_{bf} as a function of the temperature. Φ_{bf} is always larger than zero-bias barrier height ϕ_{B0} and appears at first glance to be nearly constant with as light variation. However, the flat-band barrier height Φ_{bf} is obtained to increase with decreasing temperature in a manner similar to those reported by the others [32]. Furthermore, the temperature dependence of the flat-band barrier height can be expressed as

$$\phi_{bf}(T) = \phi_{bf}(T=0) + \alpha T \tag{6}$$

where $\Phi_{bf}(T=0)$ is the zero-temperature flat-band barrier height and α is the temperature coefficient of Φ_{bf}. A plot of the flat-band barrier height Φ_{bf} as a function of the temperature is shown in Fig. 3. In Fig. 4, the fitting of $\Phi_{bf}(T)$ datain Eq. (6) yields $\Phi_{bf}(T=0)$= 1.19 eV and α = -7meV K^{-1}

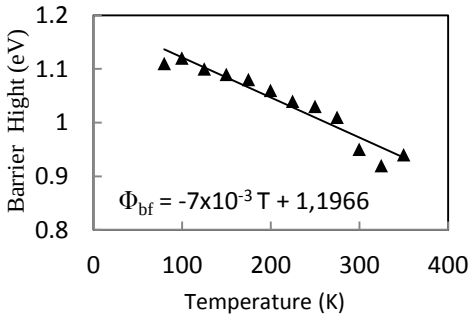

Fig. 4. Temperature dependence of flat-band barrier height for Au/n-GaP Schottky diode.

For the evaluation of the barrier height, one may also make use of the Richardson plot of the saturation current. Eq. (2) can be rewritten as

$$\ln\left(\frac{I_0}{T^2}\right)=\ln\left(AA^*\right)-\frac{q}{kT}\phi_{B0} \tag{7}$$

The dependence of$\ln(I_0/T^2)$versus $1/T$ is found tobe non-linear in the measured temperature range;however, the dependence of $\ln(I_0/T^2)$ versus $\frac{1}{nT}$gives a straight line (Fig.5). The non-linearity of the conventional $\ln(I_0/T^2)$ versus $1/T$ is caused by the temperature dependence of the barrier height and ideality factor. Similar results have also been found by several authors [6,10]. In addition, it is impossible to fit the experimental data. Theexperimental data are shown to fit asymptotically witha straight line at higher temperatures only. The values of the activation energy (E_a) and Richardson constant (A^*)were obtained from the slope and intercept of this straight-line as 0.46 eV and $1.21\text{x}10^{-7}$A/cm^2 K^{-2}, respectively. The Richardson constant value of $1.21\text{x}10^{-7}$ A/cm^2 K^{-2} is much lower than the known value of 50 A/cm^2 K^{-2} for n-GaP. Moreover, if $\ln(I_0/T^2)$ is plotted against $1/nT$, straight line is obtained with a slope giving an activation energy of 1.39 eV and this value is close to 2.37eV of GaP band gap energy, as shown in Fig. 5.

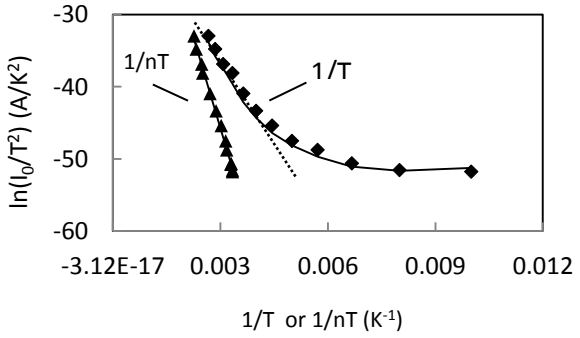

Fig. 5. Richardson plots of ln(I_0/T^2) vs. 1/T or 1/nT for Au/n-GaP Schottky diode.

The ideality factor increasing with the decreasing temperature was found to change linearly in Fig. 6 with the inverse temperature as

$$n(T)=n_0+T_0/T \tag{8}$$

where the n_0 and T_0 are constant which were found to be 0.38 and 262 K, respectively. The increase in the ideality factor with the decreasing temperature is known as T_0 effect [28].

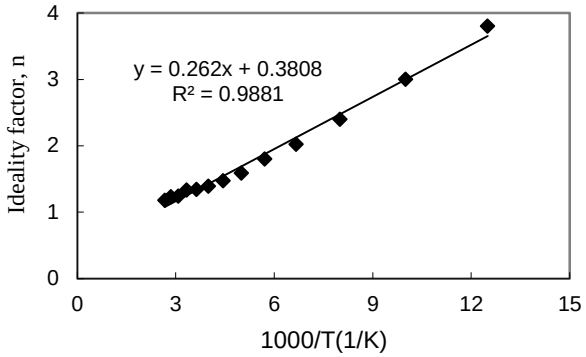

Fig. 6. The plot of n–1000/T for the Au/n-GaP Schottky barrier.

3.2. The analysis of the inhomogeneous barrier and modified Richardson plot

The above abnormal behaviors can be explained using an analytically potential fluctuation model based onspatially inhomogeneous barrier heights at the interface [6,10]. Let us assume a Gaussian distribution of the barrier heights with a mean value ϕ_{B0} and astandard deviation σ_s in the form:

$$P(\Phi_b)=\frac{1}{\sigma_S\sqrt{2\pi}}\exp\left(-\frac{(\Phi_b-\bar{\Phi}_b)^2}{2\sigma_S^2}\right) \tag{9}$$

where ϕ_{B0} denotes the mean barrier height, σ_s the standard deviation and $1/(\sigma_s\sqrt{2\pi})$ stands for the normalization constant of the Gaussian barrier height distribution. The total current through the SB at the forward bias then becomes

$$I(V)=\int_{-\infty}^{+\infty}I(\Phi_B,V)P(\Phi_B)d\Phi \tag{10}$$

where $I(\Phi_B,V)$is the current at a bias *V* for a barrier of height based on the ideal (TED) theory and P(ϕ_B) is the normalized distribution function giving the probability of accuracy for barrier height. Now integration from - ∞ to + ∞, the current *I(V)* through a Schottky barrier at a forward bias V has a similar from Eqs.(1) and (2) butwith the modified BH as, we get

$$I(V)=AA^*T^2\exp\left[-\frac{q}{kT}\left(\bar{\Phi}_B-\frac{q\sigma_S^2}{2kT}\right)\right]\exp\left(\frac{qV}{n_{ap}kT}\right)\left[1-\exp\left(\frac{-qV}{kT}\right)\right] \tag{11}$$

$$\text{With } I_o=AA^*T^2\exp\left(-\frac{q\Phi_{ap}}{kT}\right) \tag{12}$$

where ϕ_{ap} and n_{ap} are the apparent barrier height and apparent ideality factor, respectively. The assumption of the Gaussian distribution for the BH yields the following equation for the barrier height [10]

$$\Phi_{ap} = \overline{\Phi}_{Bo} - \frac{q\sigma_o^2}{2kT} \quad (13)$$

where $\overline{\Phi}_{Bo}$ is the mean SBH at zero bias and extrapolated towards zero temperature, σ_0 is the standard deviation at zero bias. In the ideal case (n =1), the expression is obtained as following suggested by [3,6,33]

$$\left(\frac{1}{n_{ap}} - 1\right) = \rho_2 - \frac{q\rho_3}{2kT} \quad (14)$$

It is assumed that the mean SBH $\overline{\Phi}_B$ and $\sigma_s$are linearly bias dependent on Gaussian parameters such as $\Phi_B = \overline{\Phi}_{Bo} - \rho_2 V$ and standard deviation $\sigma_s = \sigma_{s0} + \rho_3 V$ are voltage coefficients which may depend on T and they quantify the voltage deformation of the BH distribution. The temperature dependence of $\sigma_s$is usually small and can be neglected [6]. It is obvious that the decrease of zero-biasbarrier height is caused by the existence of the Gaussian distribution and the extent of influence is determined by the standard deviation itself. Also, the effect is particularly significant at low temperatures. Fitting of the experimental data in Eq.(2) or (12) and in Eq.(4) gives $\phi_{ap}$and n_{ap}, respectively, which should obey Eq.(13,14).

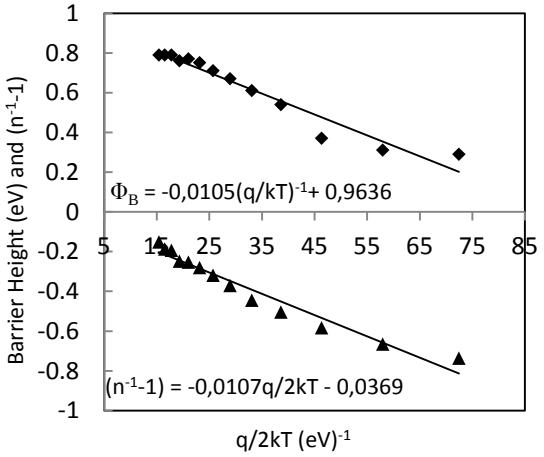

Fig. 7. Temperature dependence of barrier height (Φ_b) and ideality factor ((1/n)-1) for Au/n-GaP(100).

As can be seen from Fig. 7, the ϕ_{ap} versus $1/T$ plot should givea straight line that gives $\bar{\phi}_{B0}$and σ_0 from the intercept and slope, respectively. The experimental data in the ϕ_{ap} versus $1/T$ plot was fitted by solid line and $\bar{\phi}_{B0}$=0.97 eV and σ_0=0.10V values were obtained. According to these results, as was reported in [33] barrier

inhomogeneities can occur as a result of inhomogeneities in the composition of the interfacial oxide layer, non-uniformity of interfacial charges and interfacial oxide layer thickness. The standard deviationis also a measure of barrier homogeneity. The lower value of the σ_0 corresponds to a more homogenous BH. But the standard deviation is not small compared to mean value of 0.97 eV, and it indicates greater inhomogeneities at the interface. Potential fluctuation due to inhomogeneity affects the low temperature $I-V$ characteristics. The temperature dependence of ideality factor can be understood on the basis of Eq. (14). Fitting showing ideality factor n in Fig. 7 is a straight line that gives voltage coefficient $\rho_2$and $\rho_3$from the intercept and slope of the plot where ρ_2=-0.037 and ρ_3= 0.011 V from the experimental data. The linear behavior of the plot shows that the ideality factor expresses the voltage deformation of the Gaussian distribution of the SBD.

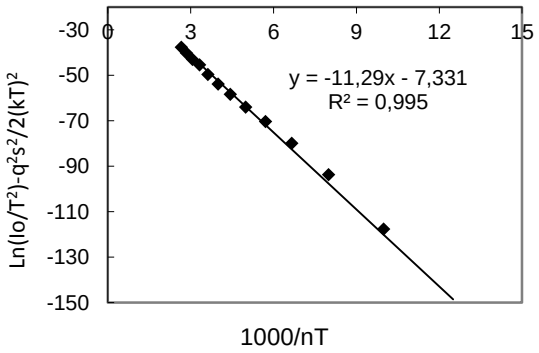

Fig. 8. Modified Richardson $\ln(I_0/T^2) - q^2\sigma_o^2/2k^2T^2$ vs 1000/Tplot for the Au/n-GaP Schottky diode according to Gaussian distribution of the barrier height.

InFig. 5, the plot of $\ln(I_0/T^2)$ versus $1/T$ plot shows that the activation energy which deviates from linearity at low temperatures. To explain this discrepancy, Eq. (10) can be rewritten by Eq. (12) with (13) as follows

$$\ln\left(\frac{I_0}{T^2}\right) - \left(\frac{q^2\sigma_o^2}{2k^2T^2}\right) = \ln(AA^*) - \frac{q\overline{\Phi}_{Bo}}{kT} \quad (15)$$

The modified $\ln(I_0/T^2) - q^2\sigma_0^2/2k^2T^2$ versus $1000/T$ plot according to Eq. (15) should give a straight line with the slope directly yielding the mean$\bar{\phi}_{B0}$ and the intercept ($lnAA^*$) at the ordinate determining A^* for a given diode area A (Fig. 8). In Fig. 8, the modified $\ln(I_0/T^2) - q^2\sigma_0^2/2k^2T^2$ versus $1000/T$ plot gives $\bar{\phi}_{B0}(T=0)$and A^* as 1.95 eV and 0.054 A cm^{-2} K^{-2},respectively. As can be seen, the value of $\bar{\phi}_{B0}(T=0)$ =1.95 eV is close to 2.37 eV of GaP band gap energy, as shown in Fig. 5. It can be seen from Fig. 8 that the modified experimental data with a good linear fit obey the barrier inhomogeneity model. Furthermore, considering a Gaussian distribution of the BHs with mean value $\bar{\phi}_{B0}$and a standard deviationσ_0 at zero bias according to [8], it can be seen that the apparent BH from the experimental forward bias I–Vplot is alsorelated to the mean BH$\bar{\phi}_{B0} = \phi_{C-V}$from the experimental reverse bias $C^{-2} - V$ plot [8]. The capacitance depends only on the mean band bending and is insensitive to the standard deviation ss of the barrier distribution [8]. The relationship between $\bar{\phi}_{B0}$ and $\phi_{C-V}$is given by:

$$\overline{\Phi}_{B0} - \Phi_{ap} = -\frac{q\sigma_o^2}{2kT} + \frac{q\alpha_\sigma}{2k} \quad (16)$$

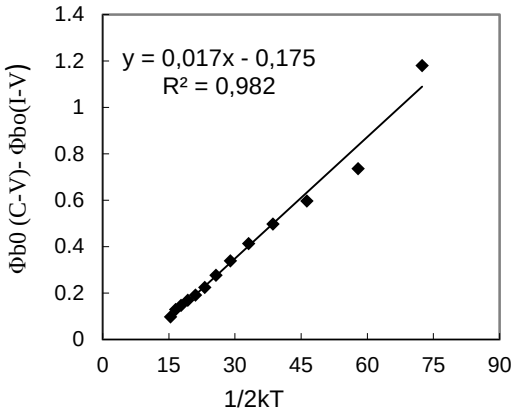

Fig. 9. The experimental ($\Phi_{c\text{-}v}$ - $\Phi_{I\text{-}V}$) vs. 1/T curves of the device according to Gaussian distribution of BHs.

Fig. 9 shows the experimental $(\phi_{C-V} - \phi_{I-V})$ versus $1/T$ plot according to Eq. (12). The plot should give a straight line of slope$\sigma_0^2 = 2k$ anda y-axis intercept $\alpha_\sigma/2k$ from which the parameters σ_0 and$\alpha_\sigma$can be determined. The slope and y-axis intercept of the plot given the values of σ_0= 0.13 Vand α_σ= 2.9x10^{-5}V^{2}K^{-1} respectively. This value of σ_0 is in close agreement with the value ofσ_0= 0.10 V from the plot of ϕ_{ap}versus $1/T$ drawn according to Eq.(13).

4. Conclusion

The current–voltage characteristics of Au/n-GaP Schottky contacts were measured in the temperaturerange 80-375 K. It is found that while the zero-bias barrier heightϕ_{B0}(I–V) increases, the ideality factor n decreases with increasing temperature. The inhomogeneities can be described by the Gaussian distribution of the barrier heights with amean barrier height $\bar{\phi}_{B0}$ =0.97 eV and standard deviation σ_0 = 0.10 V. Furthermore, the experimental results of ϕ_{ap} and n_{ap} were fitted very well with the theoretical equations related to the Gaussian distribution of ϕ_{ap} and n_{ap}. Moreover, the mean barrier height and the Richardson constant values were obtained as 1.95 eV and 0,054 A K^{-2}cm^{-2}, respectively, by means of the modified Richardson plot, $\ln(I_0/T^2) - q^2\sigma_0^2/2k^2T^2$versus $1000/T$. The value of $\bar{\phi}_{B0}(T=0)$ = 1.95 eV is close to 2.37 eV of GaP band gap energy.

References

[1] A. Singh, K. C. Reinhardt, W.A. Anderson, J. Appl. Phys. **68**, 3475 (1990).

[2] Y. P. Song, R. L. Van Meirhaeghe, W. F. Laflere, F. Cardon, Solid-state Electron. **29**, 633 (1986).

[3] S. Zeyrek, Ş. Altındal, H. Yüzer, M. M. Bülbül, Appl. Surf. Sci. **252**, 2999 (2006).

[4] S. Kar, K. M. Panchal, S. Bhattacharya, S. Varma, IEEE Trans. Electron. Devices **29**, 1839 (1982).

[5] S. Özdemir, Ş. Altındal, Solar Energy Mater. Sol. Cells **32**, 115 (1994).

[6] Ş. Karataş, Ş. Altındal, A. Türüt, A. Özmen, Appl. Surf. Sci. **217**, 250 (2003).

[7] S. Chand, J. Kumar, Semicond. Sci. Technol. **11**, 1203 (1996).

[8] J. H. Werner, H. H. Güttler, J. Appl. Phys. **69**, 1522 (1991).

[9] S. Chand, J. Kumar, J. Appl. Phys. **80**, 288 (1996); S. Chand, J. Kumar, Appl. Phys. A **63**, 171 (1996).

[10] A. Gümüş, A. Türüt, N. Yalçın, J. Appl. Phys. **91**, 245 (2002).

[11] S. Chand, Semicond. Sci. Technol. **17**, L36 (2002).

[12] S. Bandyopadhyay, A. Bhattacharya, S. K. Sen, J. Appl. Phys. **85**, 3671 (1999).

[13] B. Abay, G. Çankaya, H. S. Güder, H. Efeoğlu, Y.,K. Yoğurtçu, Semicond. Sci. Technol. **18**, 75 (2003).

[14] C. Coşkun, M. Biber, H. Efeoğlu, Appl. Surf. Sci. 211 (2003).

[15] R. F. Schmitsdorf, T. U. Kampen, W. Mönch, Surf. Sci. **324**, 249 (1995).

[16] H. Palm, M. Arbes, M. Schulz, Phys. Rev. Lett. **71**, 2224 (1993).

[17] G. M. Vanalme, L. Goubert, R. L. Van Meirhaeghe, F. Cardon, P. V. Daele, Semicond. Sci. Technol. **14**, 871 (1999).

[18] M. K. Hudait, P. Venkateswarlu, S.B. Krupanidhi, Solid-state Electron. **45**, 133 (2001).

[19] S. M. Sze, Physics of Semiconductor Devices, 2nd ed., Wiley, New York, 1981.

[20] E. H. Rhoderick, R. H. Williams, Metal–Semiconductor Contacts, Clarendon Press, Oxford, 1988.

[21] M. K. Hudait, P. Venkateswarlu, S. B. Krupanidhi, Solid State Electron. **45**, 133 (2001).

[22] Subnash, J. Kumar, Semicond. Sci. Technol. **10**, 1680 (1995).

[23] S. Chand, J. Kumar, J. Appl. Phys. **80**, 288 (1996).

[24] R. T. Tung, Phys. Rev. B **45**, 13509 (1992).

[25] R. T. Tung, Mater. Sci. Eng. R **35**, 1 (2001).

[26] E. H. Nicollian, J. R. Brews, MOS Physics and Technology, John Wiley&Sons, Newyork, 1982.

[27] R. T. Tung, Phys. Rev. B;**45**, 13509 (1992).

[28] O. Güllü, O. Barış, M. Biber, A. Türüt, Appl Surf Sci. **254**, 3039 (2008).

[29] O. Güllü, M. Biber, A. Türüt, J Mater Sci: Mater Electron. **19**, 986 (2008).

[30] S. Asubay, O. Güllü, A. Türüt Vacuum **83**, 1470 (2009).

[31] H. Doğan, H. Korkut, N. Yıldırım, A. Türüt, Appl Surf Sci. **253**, 7467 (2007).

[32] F. E. Jones, B. P. Wood, J. A. Myser, C. H. Daniels, M. C. Lonergan, J. Appl. Phys. **86**, 6431 (1999).

[33] J. H. Werner, H. H. Güttler, J. Appl. Phys. **73**, 1315 (1993).

*Corresponding author: afrailov@uludag.edu.tr